Supporting Information

Nitrogen−Rich Mesoporous Carbon Nanospheres with Atomic Fe−N_4 Sites for Efficient Oxygen Reduction

Ying Cao[a], Yiwen Cao[a], Zhiping Li[a], Sitong Qu[a], Xiaoxiao Fan[a], Xuan Wei[a,*], and Rui Cao [a,*]

a. Key Laboratory of Applied Surface and Colloid Chemistry, Ministry of Education, School of Chemistry and Chemical Engineering, Shaanxi Normal University, Xi'an 710119, China.

E−mail: weixuan@snnu.edu.cn; ruicao@snnu.edu.cn.

1. Materials characterization

Scanning electron microscopy (SEM) images were recorded on a Hitachi SU8020 microscope. Transmission electron microscopy (TEM) measurements were performed by a JEOL JEM-7900F, the acceleration voltage is 200 kV. And energy dispersive X-ray spectroscopy (EDS) was used to observe the microstructure and the uniform dispersion of C, N, O, Fe in the catalyst. Aberration-corrected High-angle annular dark field scanning transmission electron microscopic (AC-HAADF-STEM) images were performed on a FEI Themis Z transmission electron microscope operated at 200 kV, equipped with a probe spherical aberration corrector. Powder X-ray diffraction (PXRD) patterns were used to Bruker D8 Advance. Raman spectroscopy was performed on a HORIBA LabRAM Odyssey Raman spectrometer system (532 nm laser). X-ray photoelectron spectroscopy (XPS) spectra were recorded on Kratos Analytical Ltd AXIS ULTRA, N_2 adsorption-desorption isotherm and Brunauer-Emmett-Teller (BET) surface area with a Micromeritics/ASAP 2460 instrument to detect.

2. Electrochemical measurements for ORR

All electrochemical performance evaluations were carried out on the CHI 760E electrochemical workstation, utilizing a setup with three-electrode in a 0.1 M KOH solution. The carbon rod served as the counter electrode, while the Ag/AgCl electrode was used as the reference electrode. The working electrode was either a rotating disk electrode (RDE) (5 mm, 0.196 cm^2) or a rotating ring-disk electrode (RRDE) (5.61 mm, 0.247 cm^2), both coated with catalyst slurry. Among the ink of catalyst included 2 mg of the sample, 320 μL of isopropanol, 160 μL of water, and 20 μL of 5% Nafion solution, and was ultrasonicated for 1 h to obtain a homogeneous solution. The above ink was transferred 20 μL by using a pipette in twice, dropped onto the electrode surface and dried naturally at room temperature, the total load of catalyst was 0.4 mg cm^{-2}. Before testing, introducing O_2 into the 0.1 M KOH solution for 30 min to eliminate dissolved oxygen in the electrolyte. Cyclic voltammetry (CV) measurements were operated in Ar- or O_2-saturated with a scan rate of 50 mV s^{-1}. Linear sweep voltammetry (LSV) measurements were performed with a scan rate of 5 mV s^{-1} under different rotating

speeds of 400-2500 rpm after 100% IR compensation. The potentials of this experiment refer to reversible hydrogen electrode (RHE), $E_{RHE} = E_{Ag/AgCl} + 0.0592pH + 0.197$. The electron transfer number (n) was determined by RDE measurements by Koutecký-Levich (*K-L*) equation:

$$\frac{1}{j} = \frac{1}{j_1} + \frac{1}{j_k} = \frac{1}{B\omega^{1/2}} + \frac{1}{j_k}$$

$$B = 0.2nFC_0(D_0)^{2/3}v^{-1/6}$$

Where j, j_1, j_k represent the experimentally measured, diffusion limiting and kinetic current density, respectively. Ω is the rotation speed (rotations per minute, rpm), n is the electron transfer number, F is the Faraday constant (96485 C mol^{-2}), C_0 is the bulk concentration of O_2 in 0.1 M KOH ($1.2x10^{-3}$ M), D_0 is the diffusion coefficient of O_2 in 0.1 M KOH (1.9×10^{-5} cm^2 s^{-1}), and v is the kinematic viscosity (0.01 cm^2 s^{-1}). The n and hydrogen peroxide yield (H_2O_2%) also can calculated by RRDE measurements by the following equations:

$$n = \frac{4I_d}{I_d + \frac{I_r}{N}}$$

$$H_2O_2\% = \frac{200\frac{I_r}{N}}{I_d + \frac{I_r}{N}}$$

Where I_d and I_r are disk and ring current density, respectively. N is the collection efficiency of Pt ring (0.37).

3. Zn-Air battery measurements

All electrochemical performance tests of batteries were conducted on the CHI 660E electrochemical workstation. A polished round zinc plate serves as the anode of a Zinc-Air battery (thickness 0.25 mm, diameter 15 mm). And the gas diffusion layer

(thickness 0.2 mm, 1.8 x 1.8 cm^2) and the loaded catalyst layer (thickness 0.2 mm, 1.5 x 1.5 cm^2) together form the cathode of the battery. The catalyst ink was prepared as follows: 5 mg of catalyst and the baseline battery employing a mixed 2.5 mg Pt/C and 2.5 mg RuO_2 catalyst were dispersed in 910 µL of ethanol, 40 µL of water and 50 µL of Nafion (5 wt%) respectively, dissolved by ultrasound for 1 h and 500 µL of the ink was dropped onto the surface of the loaded catalyst layer, with a catalyst loading of 2 mg cm^{-2}. The electrolyte was composed of a mixture of 6 M KOH and 0.2 M $Zn(NO_3)_2 \cdot 6H_2O$. The rate capacities were evaluated by galvanostatic discharge at various current density of 2,5,10, 20 and 50 mA cm^{-2} and back to 2 mA cm^{-2}. And the cycle time of each battery was 10 min during long-term charge-discharge cycle test.

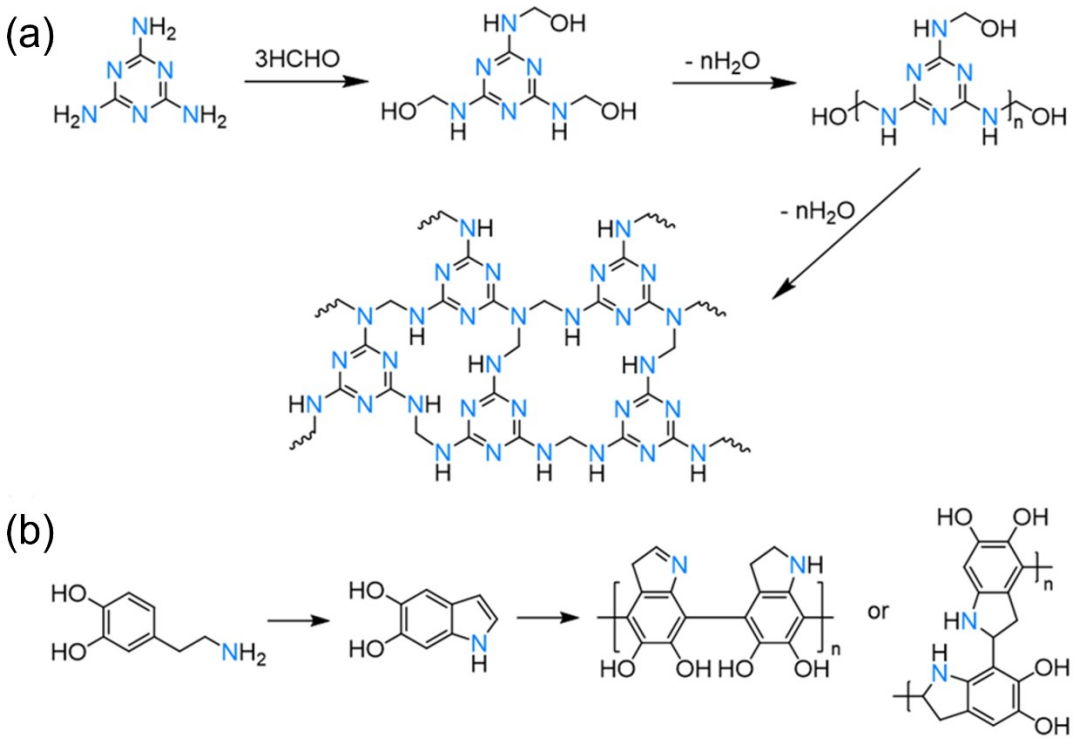

Figure S1. Structure of (a) Melamine-Formaldehyde Resin (MF resin) polymer and (b) Dopamine polymer.

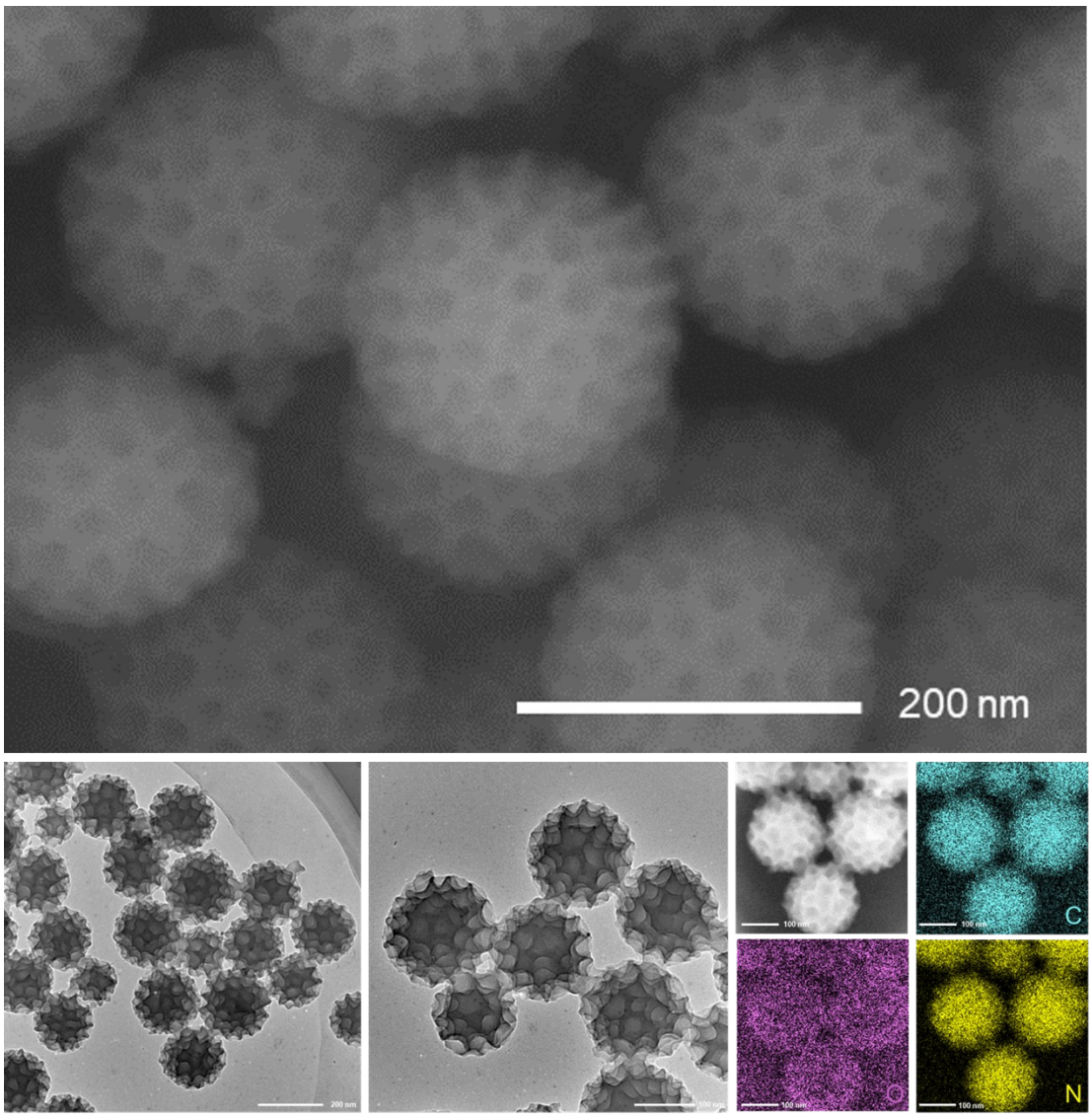

Figure S2. SEM, TEM, and EDS element maps images of the MPS.

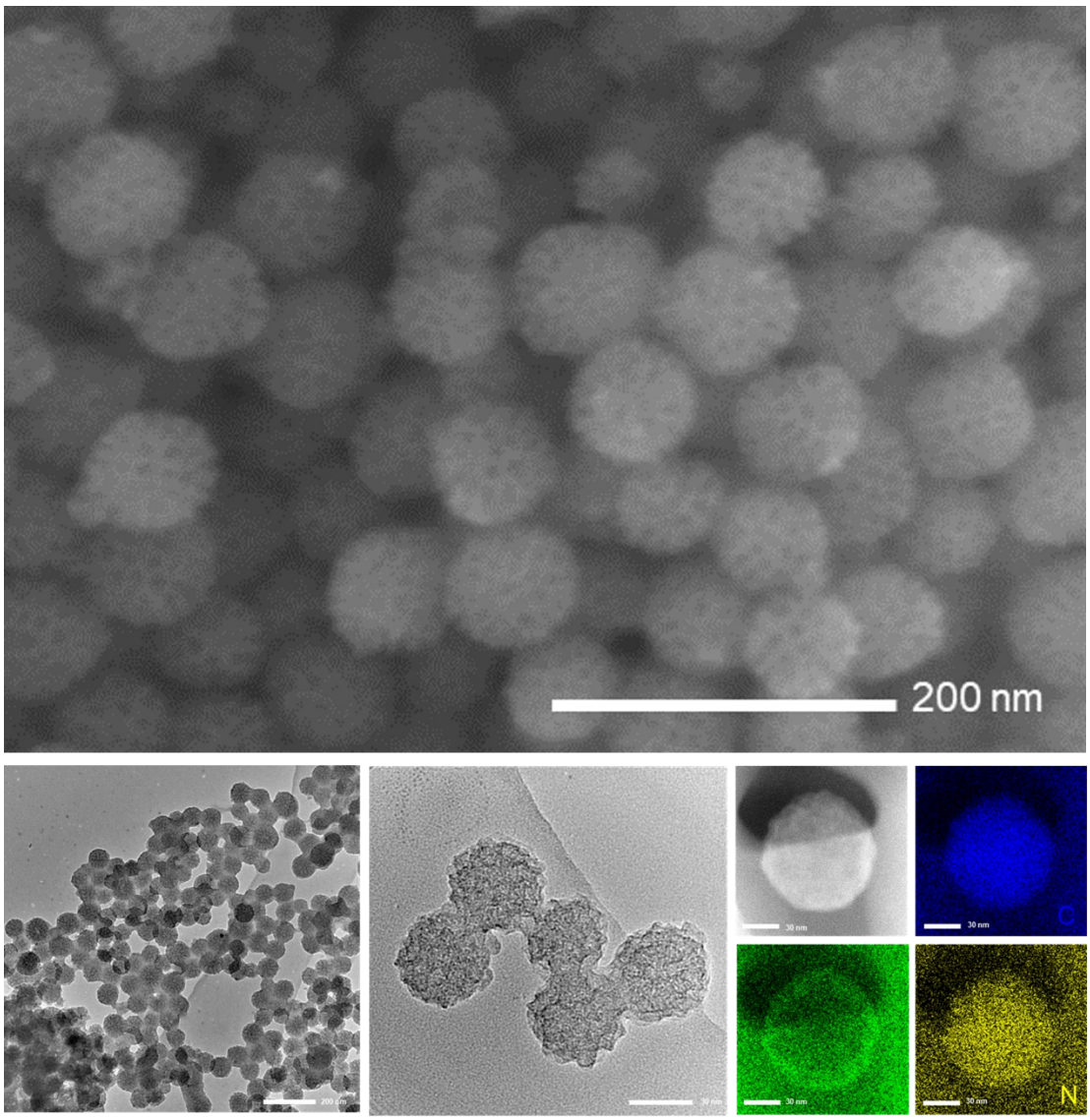

Figure S3. SEM, TEM, and EDS element maps images of the NMCSs.

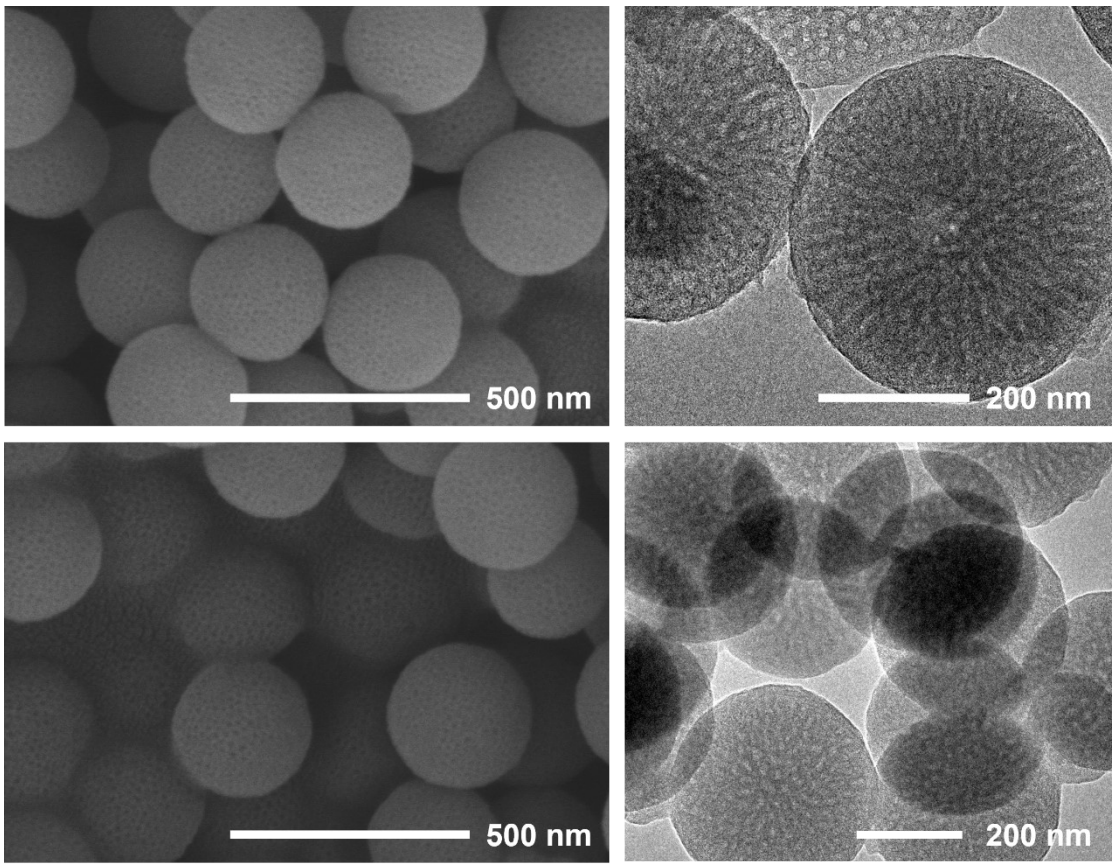

Figure S4. SEM, and TEM of the MPS (DA).

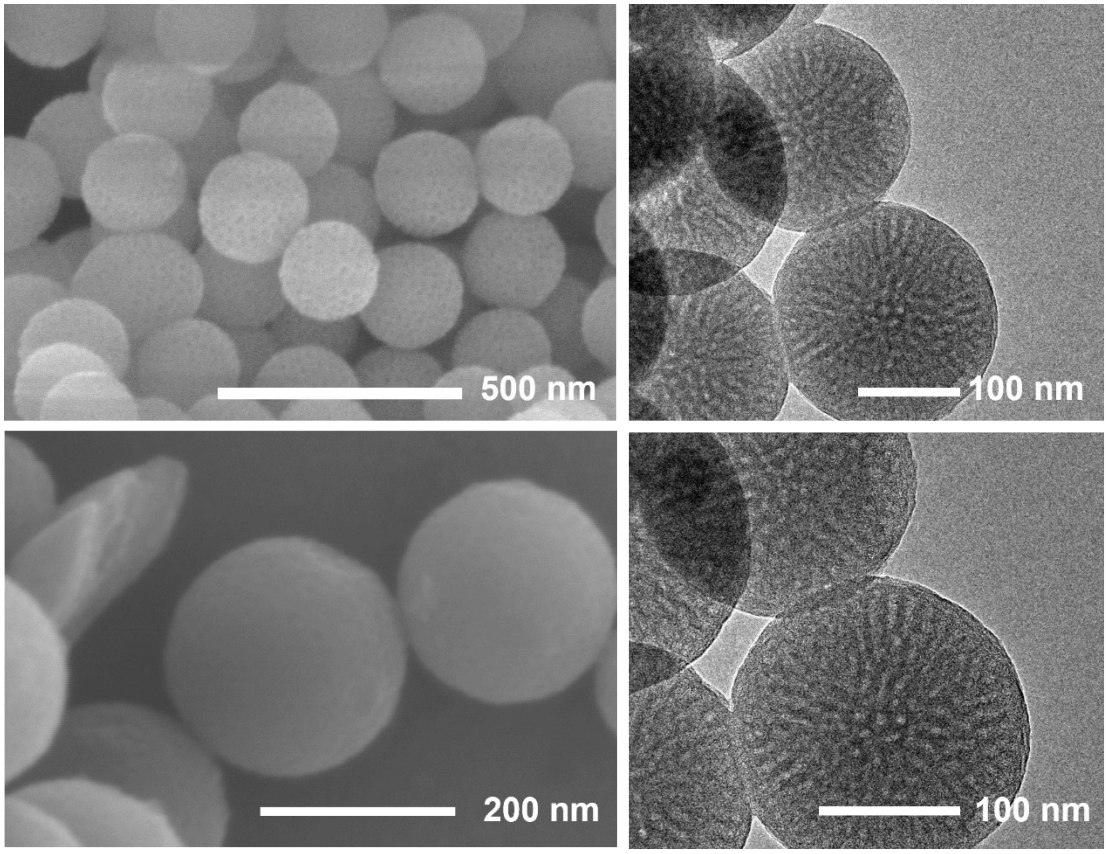

Figure S5. SEM, and TEM of the NMCSs (DA).

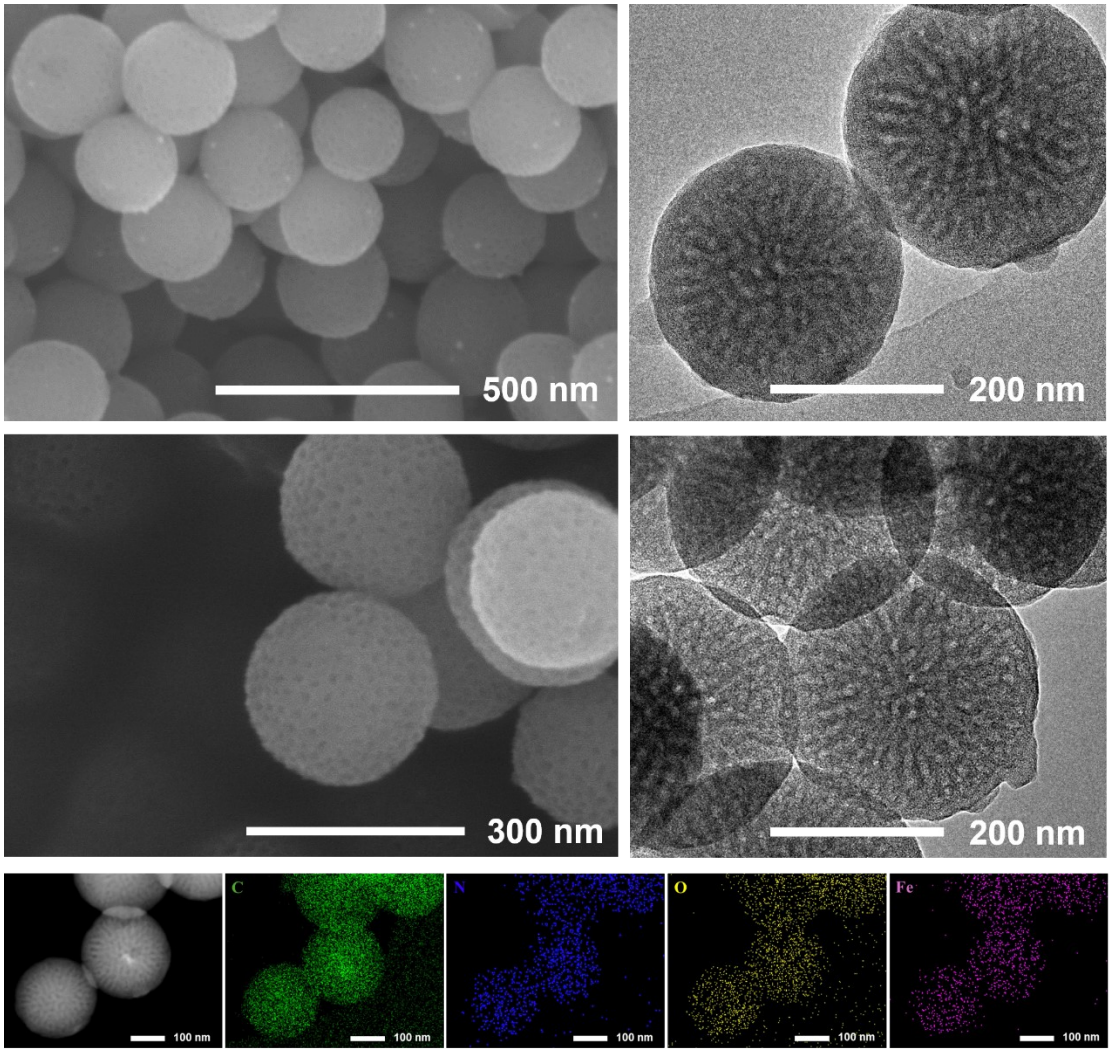

Figure S6. SEM, TEM, and EDS element maps images of the Fe-NMCSs (DA).

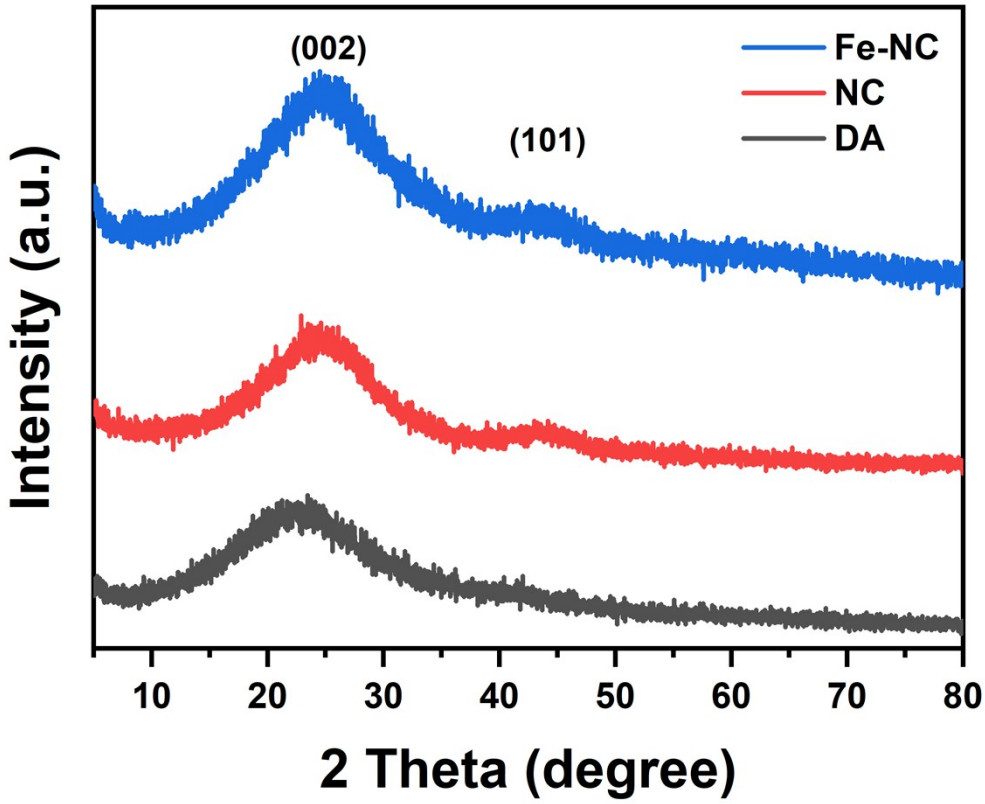

Figure S7. PXRD patterns of DA, Fe-NMCSs (DA) and NMCSs (DA).

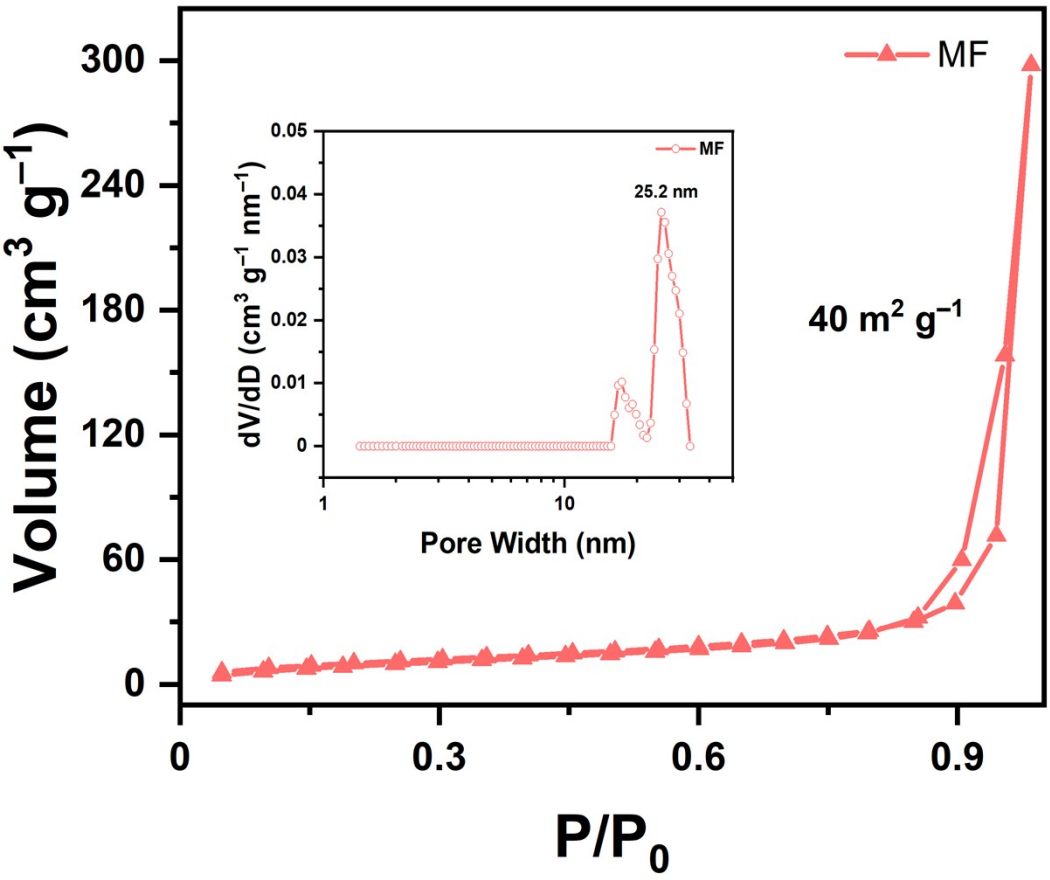

Figure S8. Nitrogen adsorption and desorption isotherm curves of MPS with the corresponding pore size distribution (inset).

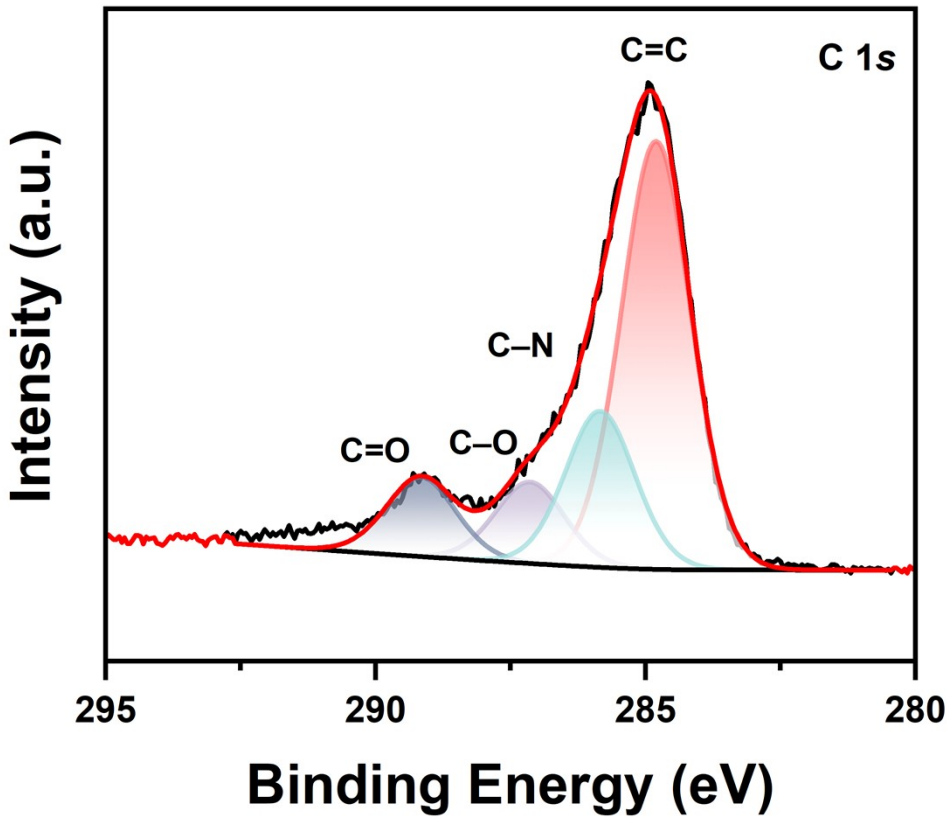

Figure S9. The C 1*s* spectrum of Fe-NMCSs.

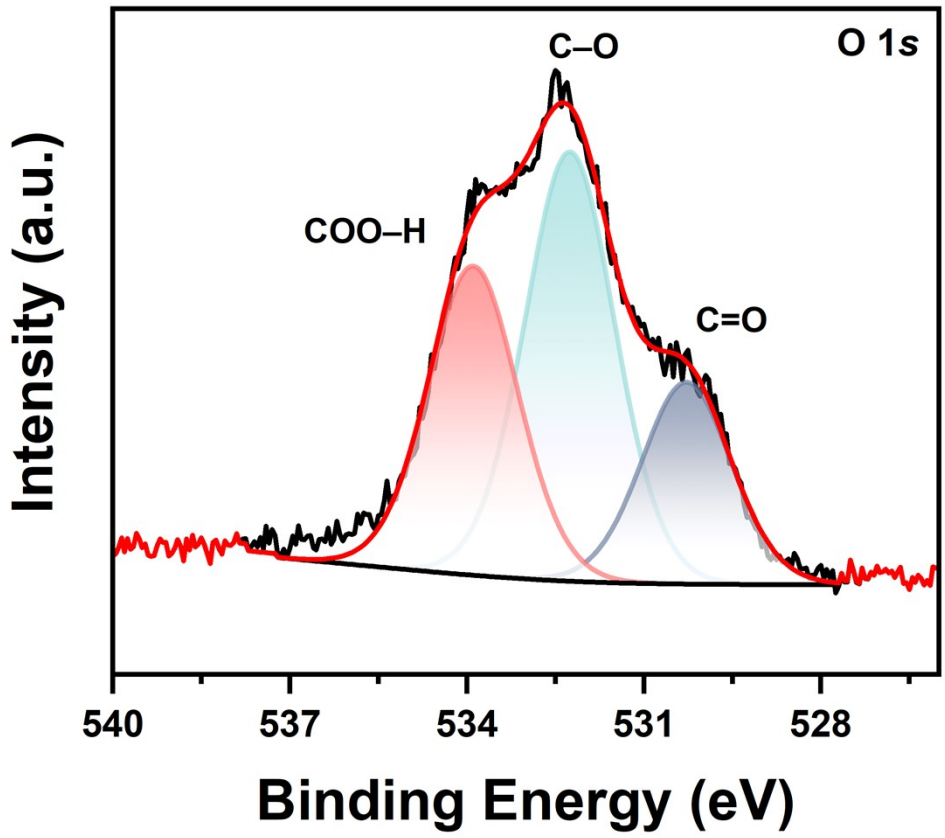

Figure S10. The O 1*s* spectrum of Fe-NMCSs.

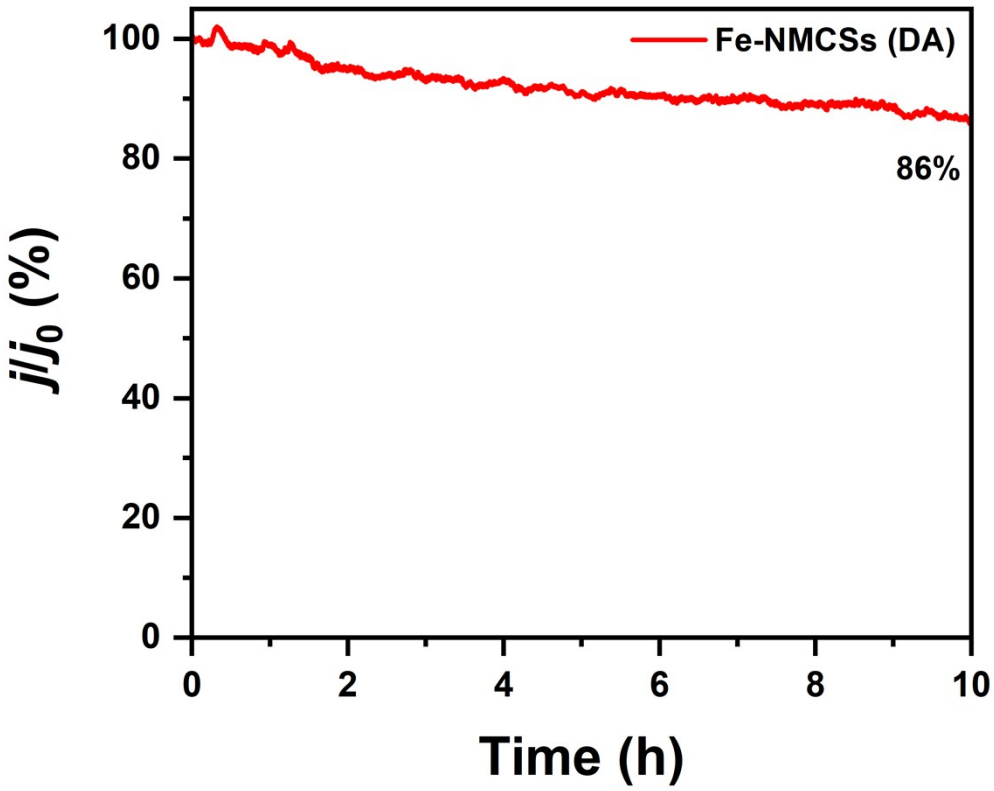

Figure S11. The stability test of Fe-NMCSs (DA) was measured at 1600 rpm in O_2-saturated 0.1 M KOH solution.

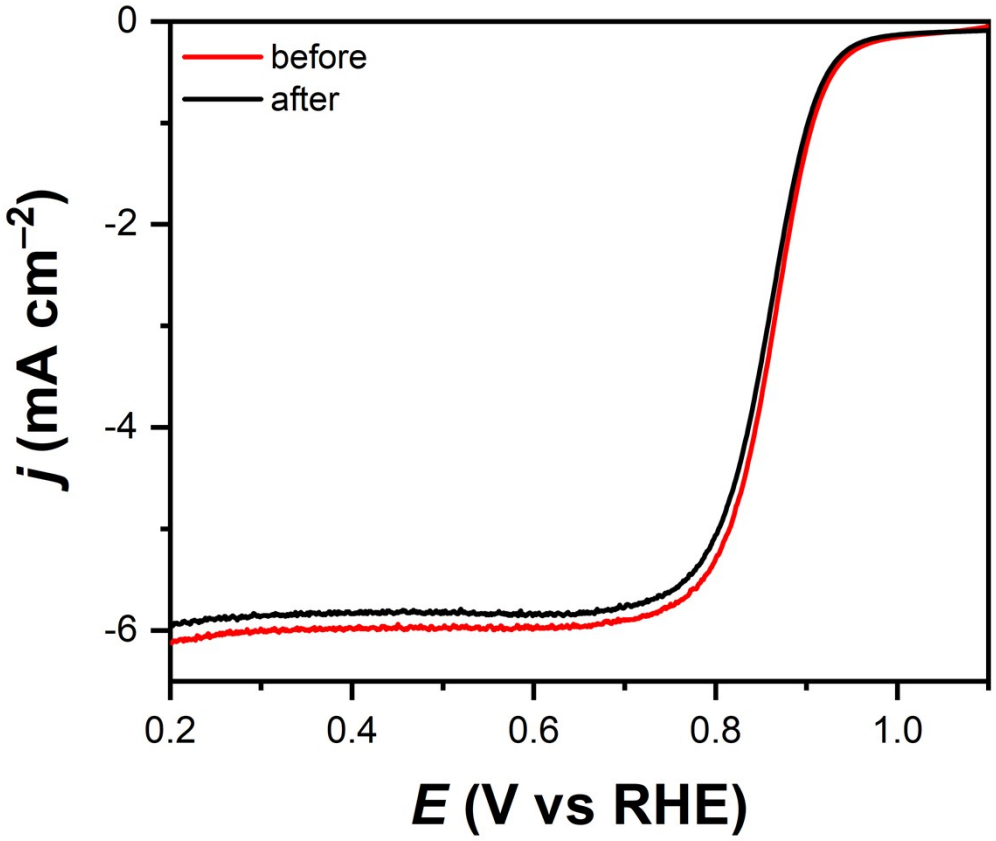

Figure S12. The LSV curve of Fe-NMCSs after 1000 CV cycles.

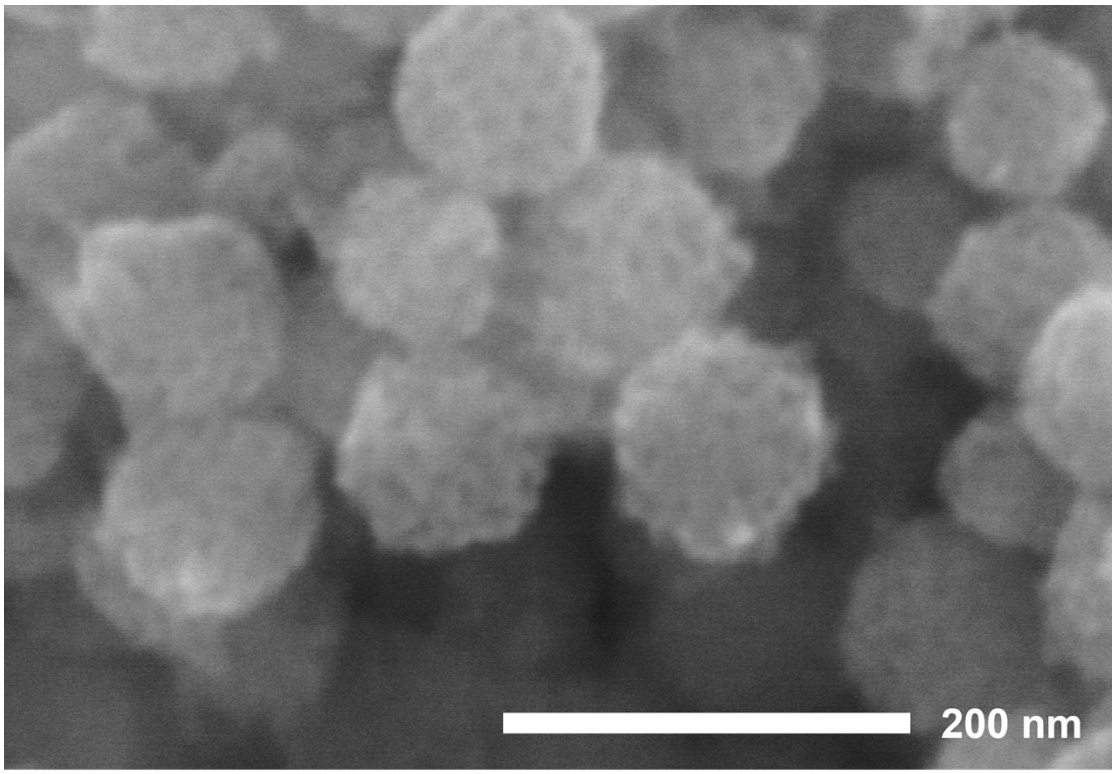

Figure S13. The SEM of post-test Fe-NMCSs.